Aalborg Universitet

AALBORG UNIVERSITY
DENMARK

Synaptic Density and Glucose Consumption in Patients with Lewy Body Diseases: An [11 C]UCB-J and [18 F]FDG PET Study

Andersen, Katrine B.; Hansen, Allan K.; Schacht, Anna Christina; Horsager, Jacob; Gottrup, Hanne; Klit, Henriette; Danielsen, Erik H.; Poston, Kathleen L.; Pavese, Nicola; Brooks, David J.; Borghammer, Per

Published in:
Movement Disorders

DOI (link to publication from Publisher):
10.1002/mds.29375

Creative Commons License
CC BY-NC-ND 4.0

Publication date:
2023

Document Version
Publisher's PDF, also known as Version of record

Link to publication from Aalborg University

Citation for published version (APA):
Andersen, K. B., Hansen, A. K., Schacht, A. C., Horsager, J., Gottrup, H., Klit, H., Danielsen, E. H., Poston, K. L., Pavese, N., Brooks, D. J., & Borghammer, P. (2023). Synaptic Density and Glucose Consumption in Patients with Lewy Body Diseases: An [11 C]UCB-J and [18 F]FDG PET Study. *Movement Disorders*, *38*(5), 796-805. Advance online publication. https://doi.org/10.1002/mds.29375

General rights
Copyright and moral rights for the publications made accessible in the public portal are retained by the authors and/or other copyright owners and it is a condition of accessing publications that users recognise and abide by the legal requirements associated with these rights.

- Users may download and print one copy of any publication from the public portal for the purpose of private study or research.
- You may not further distribute the material or use it for any profit-making activity or commercial gain
- You may freely distribute the URL identifying the publication in the public portal -

Check for updates

RESEARCH ARTICLE

Synaptic Density and Glucose Consumption in Patients with Lewy Body Diseases: An [^{11}C]UCB-J and [^{18}F]FDG PET Study

Katrine B. Andersen, MSc,[1*] Allan K. Hansen, MD, PhD,[2] Anna Christina Schacht, MSc,[1] Jacob Horsager, MD, PhD,[1] Hanne Gottrup, MD, PhD,[3] Henriette Klit, MD, PhD,[3] Erik H. Danielsen, MD, PhD,[3] Kathleen L. Poston, MD, MS,[4] Nicola Pavese, MD, PhD,[1,5] David J. Brooks, MD, DSc, FRCP, FMed Sci, FEAN,[1,5,6] and Per Borghammer, MD, PhD, DMSc[1]

[1]*Department of Nuclear Medicine and PET, Aarhus University Hospital, Aarhus, Denmark*
[2]*Department of Nuclear Medicine, Aalborg University Hospital, Aalborg, Denmark*
[3]*Department of Neurology, Aarhus University Hospital, Aarhus, Denmark*
[4]*Department of Neurology, Stanford University, Stanford, California, USA*
[5]*Translational and Clinical Research Institute, Newcastle University, Newcastle upon Tyne, UK*
[6]*Department of Brain Sciences, Imperial College London, London, UK*

ABSTRACT: Background: Patients with Lewy body diseases exhibit variable degrees of cortical and subcortical hypometabolism. However, the underlying causes behind this progressive hypometabolism remain unresolved. Generalized synaptic degeneration may be one key contributor.

Objective: The objective of this study was to investigate whether local cortical synaptic loss is proportionally linked to the magnitude of hypometabolism in Lewy body disease.

Method: Using in vivo positron emission tomography (PET) we investigated cerebral glucose metabolism and quantified the density of cerebral synapses, as measured with [^{18}F]fluorodeoxyglucose ([^{18}F]FDG) PET and [^{11}C]UCB-J, respectively. Volumes-of-interest were defined on magnetic resonance T1 scans and regional standard uptake value ratios-1 values were obtained for 14 preselected brain regions. Between-group comparisons were conducted at voxel-level.

Results: We observed regional differences in both synaptic density and cerebral glucose consumption in our cohorts of non-demented and demented patients with Parkinson's disease or dementia with Lewy bodies compared to healthy subjects. Additionally, voxel-wise comparisons showed a clear difference in cortical regions between demented patients and controls for both tracers. Importantly, our findings strongly suggested that the magnitude of reduced glucose uptake exceeded the magnitude of reduced cortical synaptic density.

Conclusion: Here, we investigated the relationship between in vivo glucose uptake and the magnitude of synaptic density as measured using [^{18}F]FDG PET and [^{11}C]UCB-J PET in Lewy body patients. The magnitude of reduced [^{18}F]FDG uptake was greater than the corresponding decline in [^{11}C]UCB-J binding. Therefore, the progressive hypometabolism seen in Lewy body disorders cannot be fully explained by generalized synaptic degeneration. © 2023 The Authors. *Movement Disorders* published by Wiley Periodicals LLC on behalf of International Parkinson and Movement Disorder Society.

Key Words: Parkinson's disease; dementia; [^{18}F]FDG PET; [^{11}C]UCB-J; synapse

This is an open access article under the terms of the Creative Commons Attribution-NonCommercial-NoDerivs License, which permits use and distribution in any medium, provided the original work is properly cited, the use is non-commercial and no modifications or adaptations are made.

***Correspondence to:** Dr. Katrine B. Andersen, Department of Nuclear Medicine and PET, Aarhus University Hospital, Palle Juul-Jensens Boulevard 165, J220, 8200 Aarhus N, Denmark;
E-mail: katrineandersen@clin.au.dk

Relevant conflicts of interest/financial disclosures: Nothing to disclose.

Funding sources: P.B. is supported by grants from the Lundbeck Foundation (R-359-2020-2533) and The Michael J. Fox Foundation (MJFF-022856).

Received: 13 December 2022; **Revised:** 2 February 2023; **Accepted:** 16 February 2023

Published online 11 March 2023 in Wiley Online Library (wileyonlinelibrary.com). DOI: 10.1002/mds.29375

Introduction

The quantitative [18F]fluorodeoxyglucose ([18F]FDG) positron emission tomography (PET) literature documents that patients with Lewy body diseases (LBD) exhibit variable degrees of hypometabolism in associative cortical regions, primary visual cortex, and to some extent in subcortical structures. The cortical hypometabolism is especially pronounced in occipital and parietal regions and ultimately in frontal regions.[1-4] In addition, it is well documented in longitudinal studies that patients with late-stage Parkinson's disease (PD) or dementia with Lewy bodies (DLB) show progressive hypometabolism,[5] which eventually becomes very pronounced. However, the underlying causes behind this progressive hypometabolism remain unresolved.

It has been hypothesized that the observed hypometabolism is explained by local cortical changes, including progressive Lewy pathology and generalized synaptic restructuring or loss.[6] Lewy pathology and synaptic loss are interrelated with glucose and energy metabolism in several ways, but the relationship needs to be further investigated.

The novel PET tracer [11C]UCB-J binds to the presynaptic vesicle protein SV2A and was in 2017 validated as the first in vivo universal synaptic density marker in humans, after confirmation of an excellent linear correlation between SV2A and the "gold standard" synaptic marker synaptophysin.[7-9] SV2A is ubiquitously expressed throughout the brain.[10] [18F]FDG PET provides a measure of cellular hexokinase activity, which reflects glucose uptake. The demand for glucose in neurons is in part driven by synaptic terminals generating ATP for the synthesis, release and recycling of neurotransmitter molecules. Therefore, [18F]FDG PET provides a validated surrogate measure of neuronal function.[11] In the present study, [18F]FDG PET was used as a measure of brain neuronal glucose uptake, to investigate the relationship between synaptic density and glucose metabolism.

The aim of this study was to investigate whether local cortical synaptic loss is proportionally linked to the magnitude of hypometabolism in Lewy body disease. Therefore, we included groups of LBD patients at different disease stages, including both non-demented patients with Parkinson's disease (nPD), and patients suffering from PD dementia (PDD) or DLB. Next, we investigated cerebral glucose metabolism and quantified the density of cerebral synapses, as measured with [18F]FDG PET and [11C]UCB-J, respectively. Previous studies have shown that patients with LBD show reduced cortical synaptic density[12] and changes in cortical metabolic function. However, we are not aware of any in vivo studies having investigated the relationship between energy metabolism and synaptic loss in the same Lewy body disease subjects.[13]

Material and Methods

Study Design and Participants

The [11C]UCB-J PET data from a total of 49 subjects, 21 nPD patients, 13 DLB/PDD patients and 15 age-matched healthy controls (HC) has been published previously.[12] In the previous study, standard uptake value ratios (SUVR)-1 values were obtained for 12 volumes-of-interest (VOI) defined on magnetic resonance imaging (MRI) T1 scans and at the voxel-level; between-group comparisons of [11C]UCB-J SUVR-1 were performed, to localize significant [11C]UCB-J binding reductions in the nPD and DLB/PDD groups compared with the 15 HCs. Finally, correlations between [11C]UCB-J PET and domain-specific cognitive functioning were examined and reported. The present study extends these analyses by the addition of [18F]FDG PET, incorporating a measure of brain metabolism and enabling investigation of the relationship between synaptic density and glucose metabolism. The study was approved by the Central Denmark Region Committees on Biomedical Research Ethics (case number 1-10-72-160-18). All 49 subjects provided informed written consent according to the Declaration of Helsinki.

In total, 49 subjects were recruited between February 2019 and December 2020, counting 21 nPD patients through the Danish PD patient society, 13 DLB/PDD patients (DLB = 9, PDD = 4) from the Movement Disorders and Memory Clinics at Aarhus University Hospital, and 15 age-matched HC subjects through advertisement in a local newspaper. All included PD subjects were on medication during the assessments (Supplementary Table S1). Table 1 presents demographic and clinical data.

The following inclusion criteria were applied as previously described[12,14]; age between 60to 85 years, at least 7 years of education and a diagnosis of either probable DLB according to consensus criteria for DLB[15] probable PDD,[16,17] PD-mild cognitive impairment (MCI) according to recently proposed diagnostic criteria,[16,18] or nPD according to Movement Disorder Society (MDS) 2015 criteria,[16] pathological [18F]FDG PET scan for DLB subjects (ie, showing occipital hypometabolism and/or the cingulate island sign) and ability to give informed consent according to the Declaration of Helsinki.

The following exclusion criteria were applied as previously described[12,14]: Montreal Cognitive Assessment (MoCA) score < 26 (for the HC group), clinical depression or clinically significant symptoms of depression (Geriatric Depression Scale [GDS-15] score >6), schizophrenia, bipolar disorder or any history of electroconvulsive therapy (ECT), past concussive head injury, stroke, major systemic diseases or medical conditions, significantly impaired hearing or sight, significant

15318257, 2023, 5, Downloaded from https://movementdisorders.onlinelibrary.wiley.com/doi/10.1002/mds.29375 by Royal Danish Library, Wiley Online Library on [22/06/2023]. See the Terms and Conditions (https://onlinelibrary.wiley.com/terms-and-conditions) on Wiley Online Library for rules of use; OA articles are governed by the applicable Creative Commons License

TABLE 1 *Demographic and clinical characteristics of study subjects*

	HC	nPD	DLB/PDD	*P*
Sample size, n	15	21	13 (9/4)	
(^{18}F)FDG	15	19	7 (3/4)	
Scanner for (^{18}F)FDG	Siemens Biograph Vision PET/CT system (HC = 15)	Siemens Biograph Vision PET/CT system (nPD = 19)	GE Discovery MI Digital Ready (DLB = 2)/Siemens Biograph Vision PET/CT system (DLB = 1, PDD = 4)	
Age	72.4 (±4.2)	71.7 (±6.4)	74.3 (±4.7)	0.35
Sex, male/female	8/7	12/9	12/1	0.06
Time since diagnosis		10.1 (±4.0)	3.8 (±5.1)	
MDS-UPDRS-III	–	26.6	26.2	
Hoehn and Yahr (1/2/3)	–	2/17/2	2/8/3	
MoCA	28.4 (27–30)	26.7 (25–28)	21.6 (18–24)	<0.001

Note: Data shown as mean ± SD or median (25%–75% quartile). *P* value refers to the overall ANOVA for all three groups.
Abbreviations: HC, healthy controls, nPD, non-demented Parkinson's disease; PDD MoCA, Parkinson's disease with dementia; DLB, dementia with Lewy bodies; FDG, fluorodeoxyglucose PET, positron emission tomography; CT, computed tomography; MDS-UPDRS-III, The Movement Disorder Society-Sponsored Revision of the Unified Parkinson's Disease Rating Scale part III; MoCA, Montreal Cognitive Assessment.

white-matter lesions observed the MRI scan (Fazekas >1), current or previous cancer, and medications affecting SV2A binding (eg, levetiracetam).

[^{18}F]FDG, [^{11}C]UCB-J PET and MRI Image Acquisition

All subjects (ie, 21 nPD patients, 13 DLB/PDD patients, and 15 age-matched HC) had [^{11}C]UCB-J PET imaging and a structural MRI. In addition, all HC (n = 15), 19 nPD, and 7 DLB/PDD had [^{18}F]FDG PET.

The healthy subjects and nPD patients all had [^{18}F]FDG PET on the Siemens Biograph Vision PET/CT system (Siemens/CTI, Knoxville, TN). Five DLB/PDD patients underwent [^{18}F]FDG PET on Siemens Biograph Vision PET/CT system and two DLB patients had [^{18}F]FDG PET on a GE Discovery MI Digital Ready camera. All participants received the three (or two) scans over a time interval of 39 ± 15 days.

All subjects received an intra-venous injection with 120 MBq (±10%) [^{18}F]FDG. A 20-minute PET acquisition was started precisely 30 minutes post-injection. Just before the [^{18}F]FDG PET acquisition, we acquired a low-dose computed tomography (CT) scan for tissue attenuation correction. Subjects had been instructed to fast for at least 4 hours before injection, and were then positioned in a quiet, dimly lit room and instructed not to speak, read, or be otherwise active after the administration of [^{18}F]FDG.

We performed tracer radiosynthesis of [^{11}C]UCB-J as described previously.[9,12,19] All 49 subjects received an intravenous bolus of 500 MBq (±10%) 60 minutes before the scan. All subjects were imaged on the ECAT Siemens High-Resolution Research Tomograph (HRRT) (Siemens/CTI, Knoxville, TN). The scan protocol included a 6-minute transmission scan followed by the 30-minute dynamic PET scan. The PET scan was attenuation corrected using the transmission scan.

All 49 subjects had MRI scans on the same 3 T Siemens SKYRA magnetic resonance system. The MRI protocol included T1- and T2-weighted MPRAGE sequences. T1 was used for co-registration with [^{11}C]UCB-J and [^{18}F]FDG PET and for VOI definition in the analysis tool PMOD 4.0. A T2 image was used to potentially exclude cases with pathology, including excessive white matter changes. No subjects were excluded.

Quantification of PET Data/Image Processing

Processing of PET images were performed using PMOD 4.0 software (PMOD4.0, PMOD technologies, Zurich, Switzerland). Pre-processing steps included image smoothing using a Gaussian kernel with a full width at half maximum of 8 mm to reduce noise at voxel level. Motion correction and frame averaging were additional steps in the pre-processing part. Other relevant toolboxes included View and Neuro tool, PMOD. Using these PMOD tools, we performed normalization of PET and MRI to Montreal Neurological Institute (MNI) space, rigid matching of each subject's PET to their representative anatomical T1 MRI, generation of uptake value ratio (SUVR) images by intensity normalization using the centrum semiovale as a reference region, MRI segmentation and VOI-based (Geometric Transfer Metrix) partial volume correction (PVC).[20,21] This PVC method was added on all our

15318257, 2023, 5, Downloaded from https://movementdisorders.onlinelibrary.wiley.com/doi/10.1002/mds.29375 by Royal Danish Library, Wiley Online Library on [22/06/2023]. See the Terms and Conditions (https://onlinelibrary.wiley.com/terms-and-conditions) on Wiley Online Library for rules of use; OA articles are governed by the applicable Creative Commons License

presented VOI data. All steps, including the VOI-based PVC were performed using the implemented toolboxes in PMOD 4.0.

White matter in the centrum semiovale has previously been validated as the preferred reference region for [11C]UCB-J PET data, therefore, making it possible to generate parametric [11C]UCB-J SUVR images.[22-25] We defined a restrictive centrum semiovale (CSO) region to minimize partial volume effects by incorporating white matter regions from Hammers atlas in PMOD using isocontours, and we included only voxels with a high probability of being part of the centrum semiovale. This resulted in a restrictive oblong CSO reference region in the center of the white matter region. Our final defined CSO region was added to the standard built-in Hammers atlas (N30R83) and applied to all 49 subjects. The defined CSO region was correspondingly used to generate comparable parametric [18F]FDG SUVR images. Therefore, all data were intensity normalized to an identical CSO reference region.

VOI regions were defined from the built-in Hammers N30R83 atlas and confirmed anatomically by overlay on the MRI scans in MNI atlas space. Some of the standard bilateral VOIs were merged to cover both left and right hemispheres, and this resulted in 14 larger composite regions including both left and right hemispheres including: anterior cingulate cortex (ACCx); cerebellum (CBL); frontal cortex (FCx); insular cortex (ICx); lateral temporal cortex (LTCx); medial temporal cortex (mTCx); occipital cortex (OCx); posterior cingulate cortex (PCCx); parietal cortex (PCx); striatum (Str); thalamus (Thal); substantia nigra (SN); amygdala (Amg); and hippocampus (Hip). The [18F]FDG uptake and [11C]UCB-J binding was then assessed in these 14 brain regions.

Statistics

We used the following statistical tools: STATA (v14.2), R (v1.1.463, RStudio, Boston, MA) and Statistical Parametric Mapping 12 (SPM12) in MATLAB 2019a. Data was assessed with Shapiro–Wilk tests, Q-Q plots, histograms, and Grubbs' test to investigate normality/normal distribution and to identify statistical outliers. We considered P values significant at a threshold of $P < 0.05$ and the Sidak-Holm method was used to correct for multiple comparisons. Group comparisons (HC, nPD, and DLB/PDD) of [11C]UCB-J SUVR-1 and [18F]FDG SUVR-1 values were assessed with a repeated measure analysis of variance (ANOVA). All three groups were compared independently using pairwise comparisons of means with equal variance (Tukey). At voxel level, unpaired t tests were performed for between group comparisons in SPM12 (cluster extent threshold k = 300 voxels, voxel size 1 × 1 × 1 mm). The surviving voxels were overlaid on a rendered brain from SPM12.

Results

The demographic and clinical characteristics of the HC, nPD, and DLB/PDD groups are presented in Table 1, in addition to an overview of scanner systems used for the [18F]FDG PET scans. Significant between group differences were observed in MoCA score ($P < 0.001$). No overall (ANOVA) between group difference were detected in age ($P = 0.36$) and sex-distribution ($P = 0.06$), although the DLB/PDD group included a higher proportion of males.

VOI Analysis

A clear average group difference was seen with respect to reduced overall [11C]UCB-J and [18F]FDG uptake in the DLB/PDD group compared to the average group image from the HC and nPD subjects (Fig. 1). A reduction in [11C]UCB-J SUVR-1 values was observed in nPD compared to HC in SN (18% loss, $P = 0.02$ uncorrected). This difference did not survive multiple comparison correction. For the DLB/PDD subjects a reduction was observed in SN (20% loss), CBL (26% loss), FCX (21% loss), ICx (46% loss), OCx (28% loss), and PCx (25% loss) when compared to the HC group. A reduction in [18F]FDG SUVR-1 values were observed in nPD compared to HC in ICx (20% loss), OCx (18% loss), PCx (14% loss) and a universal reduction in all 14 regions was observed when comparing [18F]FDG SUVR-1 values from DLB/PDD to HC (Table 2). The magnitude and spatial extent of hypometabolism as measured with [18F]FDG PET exceeded that of synaptic loss as measured by [11C]UCB-J (Fig. 1, Tables 2 and Supplementary Table S2).

Voxel-Wise Comparison

Voxel-wise comparisons in SPM12 were made between the groups for both tracers. In accordance with the reductions observed in the VOI analyses (Fig. 1, Table 2), the voxel-wise comparison showed clusters with reduced voxel values when comparing to the HC subjects (Fig. 2).

For [18F]FDG SUVR voxels, small clusters with reduced uptake was seen in posterior regions when comparing nPD and HC subjects (Fig. 2A). In contrast, no significant differences were observed in the nPD versus HC subjects in [11C]UCB-J SUVR values (Fig. 2B).

In accordance with the VOI analyses, the voxel-wise [18F]FDG SUVR comparison of DLB/PDD patients with HC showed a classical pattern of hypometabolism (Fig. 2C) including occipital, parietal, and to a lesser extent frontal regions. For [11C]UCB-J SUVR values (Fig. 2D) comparing DLB/PDD to HC subjects, considerably less extensive voxel clusters were detected in similar brain regions. The Supplementary Figure S3

15318257, 2023, 5, Downloaded from https://movementdisorders.onlinelibrary.wiley.com/doi/10.1002/mds.29375 by Royal Danish Library, Wiley Online Library on [22/06/2023]. See the Terms and Conditions (https://onlinelibrary.wiley.com/terms-and-conditions) on Wiley Online Library for rules of use; OA articles are governed by the applicable Creative Commons License

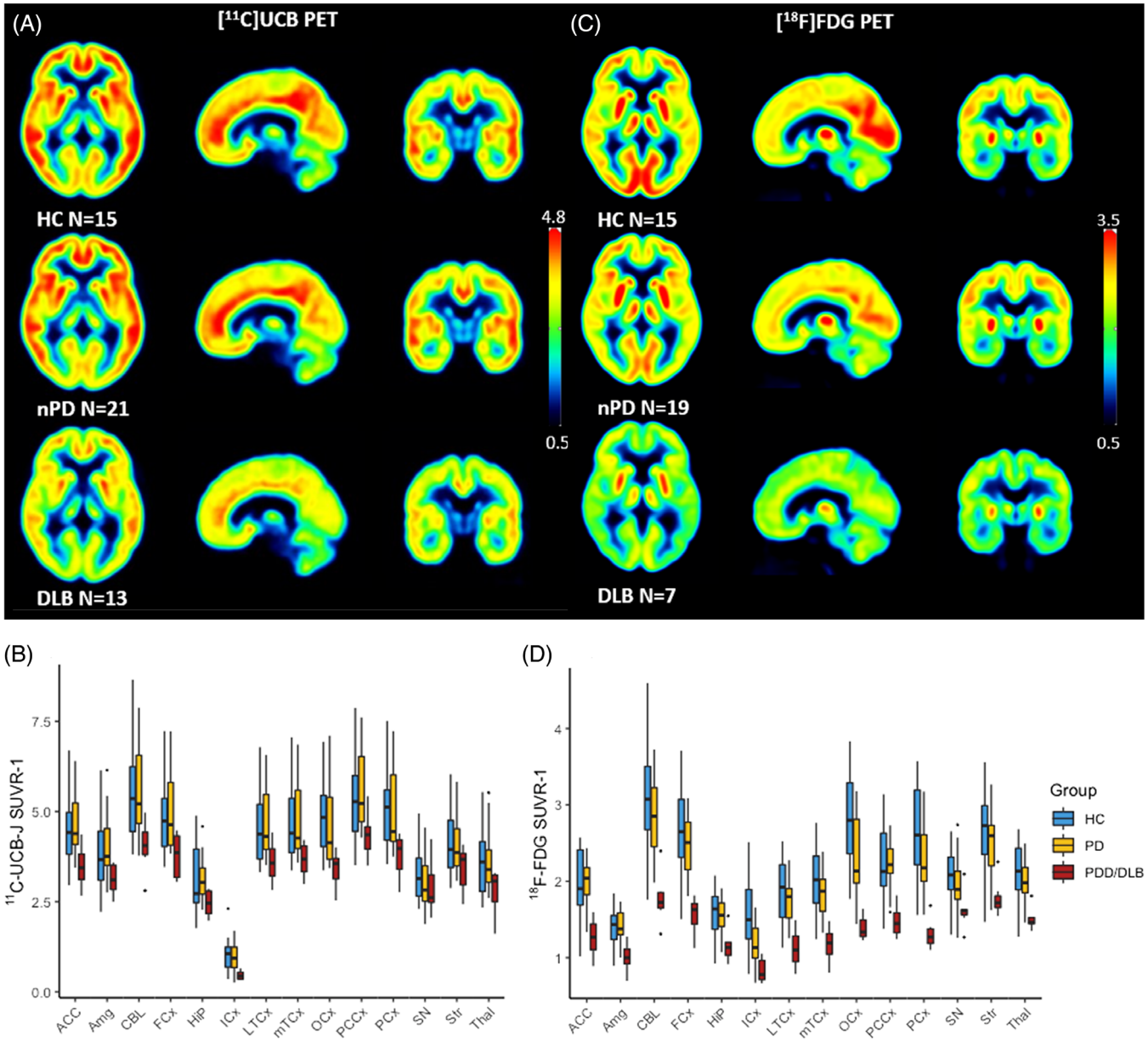

FIG. 1. (A) Average group [^{11}C]UCB-J positron emission tomography (PET) image of the brain shown for visual comparison. Color scale is standard uptake value ratios (SUVR) values. (B) Box-and-whisker plot of partial volume correction (PVC) regional [^{11}C]UCB-J binding for the healthy controls (HC) (Blue), non-demented Parkinson's disease (nPD) (yellow), and Parkinson's disease with dementia/dementia with Lewy bodies (PDD/DLB) (red). (C) Average group [^{18}F] fluorodeoxyglucose (FDG) PET image of the brain shown for visual comparison. Color scale is SUVR values. (D) Box-and-whisker plot of PVC regional [^{18}F]FDG binding for HC (blue), nPD (yellow) and PDD/DLB (red). ACCx, anterior cingulate cortex; Amg, amygdala; CBL, cerebellum; FCx, frontal cortex; Hip, hippocampus; ICx, insular cortex; LTCx, lateral temporal cortex; mTCx, medial temporal cortex; OCx, occipital cortex; PCCx, posterior cingulate cortex; PCx, parietal cortex; SN, substantia nigra; Str, striatum; Thal, thalamus. Box-and-whisker: Box contains lower quartile, upper quartile and median. Whiskers depict minimum and maximum values. [Color figure can be viewed at wileyonlinelibrary.com]

provides voxel-wise comparisons with the same voxel-based uncorrected threshold ($P = 0.001$).

Discussion

This present study explored regional and voxel level between-group differences in [^{11}C]UCB-J and [^{18}F]FDG uptake and therefore, whether synaptic loss is proportionally coupled to cerebral hypometabolism in LBD. We observed regional differences in both synaptic density and cerebral glucose consumption in our cohorts of nPD and DLB/PDD patients compared to HC subjects (Fig. 1). Additionally, our voxel-wise comparison findings showed a clear difference in cortical regions between DLB/PDD and HC for both tracers (Fig. 2). The most important finding from this study was that the magnitude and spatial extent of reduced

15318257, 2023, 5, Downloaded from https://movementdisorders.onlinelibrary.wiley.com/doi/10.1002/mds.29375 by Royal Danish Library, Wiley Online Library on [22/06/2023]. See the Terms and Conditions (https://onlinelibrary.wiley.com/terms-and-conditions) on Wiley Online Library for rules of use; OA articles are governed by the applicable Creative Commons License

TABLE 2 *Region of interest analysis of [11C]UCB-J and [18F]FDG data for HC, nPD, and DLB/PDD*

	Overall *P*	% reduction in nPD vs. HC (*P*-value)	% reduction in DLB/PDD vs. HC (*P*-value)
[11C]UCB-J CSO norm PVC			
FCX	0.022	−3 (0.47)	21 (0.04)
Hip	0.168	−1 (0.47)	18 (0.06)
Amg	0.097	−4 (0.46)	17 (0.06)
MTCx	0.051	−2 (0.47)	20 (0.05)
LTCx	0.032	−3 (0.46)	21 (0.05)
PCX	0.019	0 (0.47)	25 (0.02)
OCX	0.015	2 (0.47)	28 (0.02)
STR	0.154	0 (0.47)	17 (0.06)
SN	0.115	18 (0.09)	20 (0.06)
ICX	0.044	3 (0.46)	46 (0.03)
ACC	0.029	−4 (0.41)	20 (0.06)
PCCx	0.038	−4 (0.46)	18 (0.06)
CBL	0.014	1 (0.47)	26 (0.02)
Thal	0.080	−1 (0.47)	22 (0.06)
[18F]FDG CSO norm PVC			
FCX	0.000	7 (0.23)	38 (0.000)
Hip	0.003	4 (0.24)	24 (0.001)
Amg	0.001	−1 (0.24)	26 (0.001)
MTCx	0.000	8 (0.24)	38 (0.000)
LTCx	0.000	5 (0.23)	38 (0.000)
PCX	0.000	14 (0.07)	46 (0.000)
OCX	0.000	18 (0.02)	48 (0.000)
STR	0.003	5 (0.24)	29 (0.001)
SN	0.030	5 (0.24)	23 (0.002)
ICX	0.000	20 (0.01)	44 (0.000)
ACC	0.001	2 (0.24)	32 (0.001)
PCCx	0.001	1 (0.24)	30 (0.000)
CBL	0.000	8 (0.23)	39 (0.000)
Thal	0.001	7 (0.22)	26 (0.000)

Note: Region of interest analysis of SUVR-1 values for HC, nPD and DLB/PDD. *P* designates the overall group test *P*-value (one-way ANOVA), followed by group post-test *P*-values (pairwise comparisons of mean with equal variance). Sidak-Holm corrected values.

Abbreviations: ACCx, anterior cingulate cortex; CBL, cerebellum; CSO, centrum semiovale normalized; DLB, dementia with Lewy bodies; FCx, frontal cortex; FDG, fluorodeoxyglucose HC, healthy control; ICx, insular cortex; LTCx, lateral temporal cortex; mTCx, medial temporal cortex; nPD, non-demented Parkinson's disease; OCx, occipital cortex; PCCx, posterior cingulate cortex; PCx, parietal cortex; PVC, partial volume correction; SN, substantia nigra; Str, striatum; Thal, thalamus.

glucose uptake seems to exceed the measured reduction in cortical synaptic density. Supplementary Table S2 provides more details about the statistically comparison of the difference in mean change for [18F]FDG and [11C]UCB-J SUVR-1 s between DLB/PDD and HC subjects.

Our regional [11C]UCB-J PET findings revealed that in nPD subjects, the largest reduction in synaptic density was in the SN (18% loss). However, no significant reductions persisted after PVC and correction for multiple comparisons in this group. In contrast, DLB/PDD subjects showed significantly reduced synaptic density in most cortical regions including FCX (21% loss), ICx (46% loss), OCx (28% loss), PCx (25% loss), and CBL (28% loss) when compared to the HC group (Table 2).

Our regional [18F]FDG findings showed significant reductions in ICx, OCx, and PCx when comparing nPD patients to the HC group. Additionally, a universal [18F]FDG reduction of larger magnitude was seen across all 14 regions when comparing the DLB/PDD patients to the HC group. Together, these volume of interest data show a larger percentage reduction in [18F]FDG uptake compared to [11C]UCB-J PET (Fig. 1 and Table 2). Our voxel-wise comparison findings further corroborated these findings, by showing clear differences in cortical reduction of [18F]FDG uptake compared to the minor reduction observed in [11C]UCB-J binding (Fig. 2). Although the differences in [18F]FDG SUVR values between nPD and HC subjects were only small and sporadic, it still showed a greater reduction of glucose metabolism compared to the reduction in synaptic density. This difference was even more pronounced in the PDD/DLB group (Fig. 2C).

To date, several studies have verified a disease-specific hypometabolism pattern for PD and PDD/DLB patients.[26-29] Such studies have investigated subgroups of cognitive impaired and demented PD patients and reported extensive hypometabolism in cortical areas including general parietooccipital and frontal areas. Our [18F]FDG PET data (Fig. 2C) resembled the well-known cortical pattern of hypometabolism seen in these patients, supporting the validity of our findings.

Two recent studies have identified synaptic density alterations in PDD/DLB patients with the use of [11C]UCB-J PET,[12,30] but no studies have investigated whether synaptic density is related to cerebral glucose metabolism measured with [18F]FDG PET within these patients. One recently published study investigated [11C]UCB-J binding and [18F]FDG PET uptake in patients with Alzheimer's disease (AD). They found more pronounced hypometabolism measured with [18F]FDG PET compared to synaptic loss within cortical brain area and comparable [18F]FDG PET and [11C]UCB-J reduction in medial temporal regions.[31] Another recent study investigated this relationship in the

15318257, 2023, 5, Downloaded from https://movementdisorders.onlinelibrary.wiley.com/doi/10.1002/mds.29375 by Royal Danish Library, Wiley Online Library on [22/06/2023]. See the Terms and Conditions (https://onlinelibrary.wiley.com/terms-and-conditions) on Wiley Online Library for rules of use; OA articles are governed by the applicable Creative Commons License

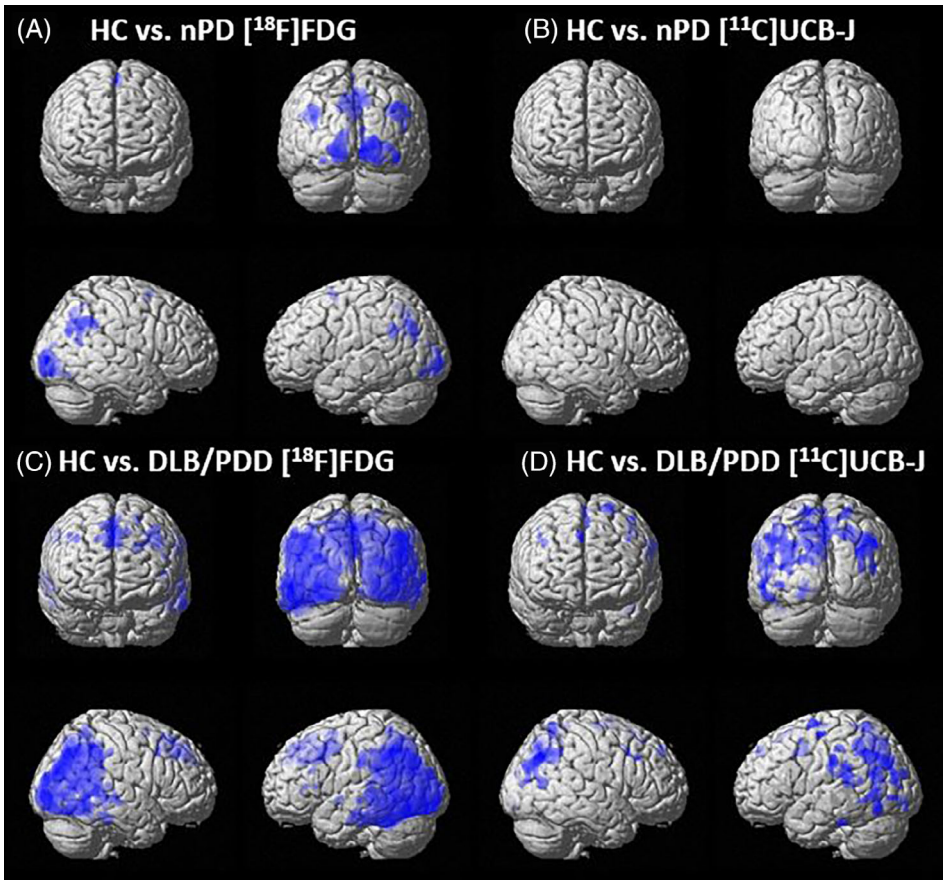

FIG. 2. (A) Comparison of healthy controls (HC) (n = 15) and non-demented Parkinson's disease (nPD) (n = 19) [^{18}F] fluorodeoxyglucose (FDG) standard uptake value ratios (SUVR) (voxel: $P = 0.01$ unc with cluster thresholding, k = 300 voxels). (B) Comparison of HC (n = 15) and nPD (n = 21) [^{11}C]UCB-J SUVR (voxel: $P = 0.01$ unc with cluster thresholding, k = 300 voxels). (C) Comparison of HC (n = 15) and Parkinson's disease with dementia/dementia with Lewy bodies (PDD/DLB) (n = 7) [^{18}F]FDG SUVR (voxel: $P = 0.0001$ unc with cluster thresholding, k = 300 voxels). (D) Comparison of HC (n = 15) and PDD/DLB (n = 13) [^{11}C]UCB-J SUVR (voxel: $P = 0.0001$ unc with cluster thresholding, k = 300 voxels). [Color figure can be viewed at wileyonlinelibrary.com]

cortico–striato–thalamo–cortical circuit following a unilateral dopaminergic lesion in rats and compared to sham lesioned rats.[13] They reported hypometabolism in motor and orbitofrontal cortex measured with [^{18}F]FDG PET,[13] but synaptic loss measured with [^{11}C]UCB-J PET was not demonstrated in these regions. Accordingly, these findings also suggest a greater degree of hypometabolism compared to synaptic loss in these patients and experimental animals, but also that alterations in synaptic density and metabolism can be regionally divergent within the brain. Of interest, a recent study of patients with Huntington's disease revealed spatially more extensive reductions in [^{11}C]UCB-J PET uptake compared to [^{18}F]FDG uptake.[32] Whereas the above mentioned study in AD reported similar findings to our results in DLB[31] (ie, more widespread [^{18}F]FDG reductions compared to UCB-J.) These discrepancies are interesting and suggest that the degree of hypometabolism does not exceed synaptic loss in all neurodegenerative diseases. Perhaps the preferential loss of inhibitory medium spiny neurons in Huntington's disease could lead to a disinhibitory state, which would not be followed by downstream hypometabolism. The availability of synaptic PET tracers now allows such hypotheses to be explored.

Our findings were in line with the previously published study in AD[31] and in rodents.[13] When testing if the observed percentage reduction in our DLB/PDD patients was significantly larger in [^{18}F]FDG uptake compared to the reduction in [^{11}C]UCB-J binding, we revealed that the magnitude of hypometabolism was significantly greater within all cortical brain areas (except for the ICx), whereas similar reductions were observed in medial temporal regions including HIP, Amg, Thal, and additionally SN (Table S2). In brief, this finding suggested a regional decoupling of synaptic density and metabolism in the DLB/PDD patients. This regional divergence could be explained by several factors, including alterations in local perfusion and metabolism in response to changes in neuronal/synaptic activity, regionally abnormal protein aggregation, regionally altered synaptic plasticity, and degradation of important subcortical neuromodulatory systems in LBDs.

15318257, 2023, 5, Downloaded from https://movementdisorders.onlinelibrary.wiley.com/doi/10.1002/mds.29375 by Royal Danish Library, Wiley Online Library on [22/06/2023]. See the Terms and Conditions (https://onlinelibrary.wiley.com/terms-and-conditions) on Wiley Online Library for rules of use; OA articles are governed by the applicable Creative Commons License

Therefore, our present study demonstrates that the percentage decrease in [18F]FDG uptake significantly exceeded that of the percentage loss of synaptic density in Lewy body patients in most regions except SN, Thal, HIP, Amg, and ICx (Tables 2 and S2). This supports the idea that synaptic dysfunction precedes synaptic loss. There may be several possible explanations for this disproportionally larger magnitude of hypometabolism.

First, LBD are neurodegenerative disorders involving degenerative alterations in numerous neurobiological processes, including synaptic changes and perturbed metabolism.[33-35] Therefore, the reduced glucose hypometabolism observed in these patients may to some extent be explained by general neurodegeneration.

Second, it is possible that cortical hypometabolism observed in these patients may in part be caused by degeneration of important subcortical neuromodulatory systems. PD is a multi-system disorder, which in addition to the well-known degeneration of dopaminergic neurons in the SN is also characterized by degeneration of several other subcortical systems, including noradrenergic neuronal loss in the locus coeruleus,[36-39] degeneration of serotonergic neurons of the dorsal raphe nuclei[40-43] and of cholinergic neurons of the nucleus basalis of Meynert,[39,44-47] as well as other nuclei including the ventral tegmental area[48] and pedunculopontine nucleus.[49,50] Several studies have investigated these subcortical systems and have generally reported an activating (excitatory) effect of these systems on the cerebral cortex.[51-54] Therefore, neuron loss and dysfunction in these subcortical systems could very plausibly result in widespread hypometabolism across the cortex.[55] Interestingly, one study reported cholinergic loss to start posteriorly in PD cases and spread anteriorly in PDD, corresponding to the documented patterns of progressive reductions in [18F]FDG uptake.[56]

Finally, it is interesting to note that whereas some colocalization between cortical hypometabolism and Lewy body pathology exists,[57,58] the patterns are far from identical. In particular, hypometabolism is very pronounced in occipital cortex, which generally shows relatively sparse Lewy pathology in postmortem studies.[55,58] This further supports the proposal that cortical hypometabolism may be caused by a combination of cortical and subcortical pathologies in Lewy body disorders.

Our findings should be interpreted with caution and the study had several limitations. First, the sample size was very modest. Particularly the sample size of our DLB/PDD group was limited with only seven patients with [18F]FDG PET. Consequently, we controlled for multiple comparisons and limited the number of analyses, to deal with our limited statistic power.

Second, several studies have confirmed that the CSO is a valid reference region for [11C]UCB-J PET intensity normalization and that grey matter/white matter ratios are proportional to volume-of-distribution parameters.[22-25] Of note, one previous study did report 10% to 20% SV2A specific binding of [11C]UCB-J in CSO[7]. Furthermore, several studies have shown that glucose uptake as measured with [18F]FDG PET is stable in white matter[55,59] and well preserved in PD,[60] if care is taken to only include the centermost part of white matter and therefore, avoiding partial volume effects. Nevertheless, white matter is a different tissue class compared to gray matter, and may therefore, not be optimal as a reference region for either [11C]UCB-J PET or [18F]FDG PET. Therefore, the definition of the reference region CSO and its proximity to other tissue classes (ie, grey matter and cerebrospinal fluid) could influence and potentially bias our SUVR data. In addition, we calculated SUVR-1 values for both [18F]FDG and [11C]UCB-J, but these may not be directly comparable. For [11C]UCB-J, SUVR-1 approximates the ratio between specific and non-specific binding such that an SUVR-1 of zero suggests a complete absence of SV2A and hence, of synapses. For [18F]FDG, SUVR-1 designates how much grey matter metabolism exceeds white matter metabolism in a relative sense, so here, an SUVR-1 of zero does not mean the absence of metabolism, but rather that grey matter metabolism is equal to white matter metabolism. Therefore, the present results should preferably be reproduced with full kinetic modeling of [18F]FDG PET data.

Third, it cannot be excluded that atrophy may have affected our results, even after PVC. Therefore, a possible partial volume effect must be mentioned as a limitation, although our results suggest that any effects of atrophy were probably minor. Moreover, any such effect would probably affect both the [18F]FDG and [11C]UCB-J data to a similar degree and therefore, be less of a problem when comparing the relationship between these tracers.

Fourth, all our included patients, except two of our DLB patients, were on medication including levodopa, Ma-B inhibitors, dopamine agonist or AchE inhibitors (Supplementary Table **S1**). None of our DLB patients were on Parkinson specific medication such as levodopa. Some studies have suggested a promoting effect of levodopa on synaptic plasticity and transmission, which would hypothetically trigger an increase of SV2A expression levels and therefore, [11C]UCB-J binding in our levodopa treated nPD patients. Accordingly, this may have caused an underestimation of the observed difference between nPD and HC. In addition, 11/13 of our DLB/PDD patients were on AChE inhibitors. It seems unlikely that AChE inhibitors would have any major effects on the overall density of synapses, which could alter findings on [11C]UCB-J PET, but to our knowledge, this has not been studied. Regarding [18F]FDG PET, 5/7 of our DLB/PDD patients were on AChE

15318257, 2023, 5, Downloaded from https://movementdisorders.onlinelibrary.wiley.com/doi/10.1002/mds.29375 by Royal Danish Library, Wiley Online Library on [22/06/2023]. See the Terms and Conditions (https://onlinelibrary.wiley.com/terms-and-conditions) on Wiley Online Library for rules of use; OA articles are governed by the applicable Creative Commons License

inhibitors. Some studies have suggested a minor excitatory effect of AChE inhibitors on brain metabolism, which would in theory result in higher [^{18}F]FDG uptake in our DLB/PDD group.[61] Accordingly, the magnitude of hypometabolism seen in our DLB/PDD group could have been underestimated.

Finally, two different PET systems were used during [^{18}F]FDG PET to image the DLB/PDD groups, which may have contributed to some dissimilarities during analysis in PMOD. However, no apparent differences in the pattern or magnitude of [^{18}F]FDG uptake were detected manually between the two PET cameras during the analyses in PMOD. In addition, all UCB-J PET scans were performed on the ECAT Siemens High-Resolution Research Tomograph (HRRT) (Siemens/CTI, Knoxville, TN, USA), whereas 39/41 (95%) of FDG scans were done on a Siemens biograph Vision PET/CT system. The HRRT has slightly better spatial resolution compared to the Vision, whereas the Vision uses more modern reconstruction algorithms and excellent time-of-flight methodology. The end result is remarkably similar image quality in PET images from the HRRT and Vision cameras. Additionally, all image volumes were filtered with an 8 mm Gaussian filter. Any differences in quantitative values of the two images were most likely relatively minor.

In conclusion, our study investigated the relationship between in vivo glucose uptake and the magnitude of synaptic density as measured using [^{18}F]FDG PET and [^{11}C]UCB-J PET for the first time in Lewy body patients (PD and DLB/PDD). The magnitude of reduced [^{18}F]FDG uptake was greater than the corresponding decline in [^{11}C]UCB-J binding, which was seen in both VOI and voxel-based analysis. Therefore, the magnitude of reduced [^{18}F]FDG uptake seen in Lewy body disorders probably cannot be fully explained by local synaptic loss. We hypothesize that cortical hypometabolism in Lewy body disorders could in part be caused by neurodegeneration of subcortical modulatory, ascending neurotransmitter systems, which could result in the loss of a generally excitatory drive on the cortex. This theory could be explored in animal studies by quantifying the relative loss of [^{11}C]UCB-J and [^{18}F]FDG signal after standardized lesioning of different neurotransmitter systems or by using transgene animal models overexpressing a-synuclein. ●

Acknowledgment: We thank all participants for their willingness to participate in our study.

Data Availability Statement

The data that support the findings of this study are available from the corresponding author upon reasonable request.

References

1. Huang C, Mattis P, Perrine K, Brown N, Dhawan V, Eidelberg D. Metabolic abnormalities associated with mild cognitive impairment in Parkinson disease. Neurology 2008;70(16):1470–1477.
2. Huang C, Mattis P, Tang C, Perrine K, Carbon M, Eidelberg D. Metabolic brain networks associated with cognitive function in Parkinson's disease. Neuroimage 2007;34(2):714–723.
3. Liepelt I, Reimold M, Maetzler W, et al. Cortical hypometabolism assessed by a metabolic ratio in Parkinson's disease primarily reflects cognitive deterioration-[18F]FDG-PET. Mov Disord 2009;24(10):1504–1511.
4. Hosokai Y, Nishio Y, Hirayama K, et al. Distinct patterns of regional cerebral glucose metabolism in Parkinson's disease with and without mild cognitive impairment. Mov Disord 2009;24(6):854–862.
5. Kapitan M, Ferrando R, Dieguez E, et al. Regional cerebral blood flow changes in Parkinson's disease: correlation with disease duration. Rev Esp Med Nucl 2009;28(3):114–120.
6. Kramer ML, Schulz-Schaeffer WJ. Presynaptic alpha-synuclein aggregates, not Lewy bodies, cause neurodegeneration in dementia with Lewy bodies. J Neurosci 2007;27(6):1405–1410.
7. Finnema SJ, Nabulsi NB, Eid T, et al. Imaging synaptic density in the living human brain. Sci Transl Med 2016;8(348):348ra396.
8. Finnema SJ, Nabulsi NB, Mercier J, et al. Kinetic evaluation and test-retest reproducibility of [(11)C]UCB-J, a novel radioligand for positron emission tomography imaging of synaptic vesicle glycoprotein 2A in humans. J Cereb Blood Flow Metab 2018;38(11):2041–2052.
9. Nabulsi NB, Mercier J, Holden D, et al. Synthesis and preclinical evaluation of 11C-UCB-J as a PET tracer for imaging the synaptic vesicle glycoprotein 2A in the brain. J Nucl Med 2016;57(5):777–784.
10. Bajjalieh SM, Frantz GD, Weimann JM, McConnell SK, Scheller RH. Differential expression of synaptic vesicle protein 2 (SV2) isoforms. J Neurosci 1994;14(9):5223–5235.
11. Attwell D, Iadecola C. The neural basis of functional brain imaging signals. Trends Neurosci 2002;25(12):621–625.
12. Andersen KB, Hansen AK, Damholdt MF, et al. Reduced synaptic density in patients with Lewy body dementia: an [(11) C]UCB-J PET imaging study. Mov Disord 2021;36(9):2057–2065.
13. Raval NR, Gudmundsen F, Juhl M, et al. Synaptic density and neuronal metabolic function measured by positron emission tomography in the unilateral 6-OHDA rat model of Parkinson's disease. Front Synaptic Neurosci 2021;13:715811.
14. Andersen KB, Hansen AK, Knudsen K, et al. Healthy brain aging assessed with [(18)F]FDG and [(11)C]UCB-J PET. Nucl Med Biol 2022;112-113:52–58.
15. McKeith IG, Boeve BF, Dickson DW, et al. Diagnosis and management of dementia with Lewy bodies: fourth consensus report of the DLB consortium. Neurology 2017;89(1):88–100.
16. Postuma RB, Berg D, Stern M, et al. MDS clinical diagnostic criteria for Parkinson's disease. Mov Disord 2015;30(12):1591–1601.
17. Goetz CG, Emre M, Dubois B. Parkinson's disease dementia: definitions, guidelines, and research perspectives in diagnosis. Ann Neurol 2008;64(Suppl 2):S81–S92.
18. Litvan I, Goldman JG, Troster AI, et al. Diagnostic criteria for mild cognitive impairment in Parkinson's disease: Movement Disorder Society Task Force guidelines. Mov Disord 2012;27(3):349–356.
19. Thomsen MB, Schacht AC, Alstrup AKO, et al. Preclinical PET studies of [(11)C]UCB-J binding in minipig brain. Mol Imaging Biol 2020;22(5):1290–1300.
20. Rousset OG, Collins DL, Rahmim A, Wong DF. Design and implementation of an automated partial volume correction in PET: application to dopamine receptor quantification in the normal human striatum. J Nucl Med 2008;49(7):1097–1106.
21. Rousset OG, Ma Y, Evans AC. Correction for partial volume effects in PET: principle and validation. J Nucl Med 1998;39(5):904–911.

15318257, 2023, 5, Downloaded from https://movementdisorders.onlinelibrary.wiley.com/doi/10.1002/mds.29375 by Royal Danish Library, Wiley Online Library on [22/06/2023]. See the Terms and Conditions (https://onlinelibrary.wiley.com/terms-and-conditions) on Wiley Online Library for rules of use; OA articles are governed by the applicable Creative Commons License

22. Koole M, van Aalst J, Devrome M, et al. Quantifying SV2A density and drug occupancy in the human brain using [(11)C]UCB-J PET imaging and subcortical white matter as reference tissue. Eur J Nucl Med Mol Imaging 2019;46(2):396–406.
23. Mercier J, Provins L, Valade A. Discovery and development of SV2A PET tracers: potential for imaging synaptic density and clinical applications. Drug Discovery Today Technol 2017;25:45–52.
24. Mertens N, Maguire RP, Serdons K, et al. Validation of parametric methods for [(11)C]UCB-J PET imaging using subcortical White matter as reference tissue. Mol Imaging Biol 2020;22(2):444–452.
25. Rossano S, Toyonaga T, Finnema SJ, et al. Assessment of a white matter reference region for (11)C-UCB-J PET quantification. J Cereb Blood Flow Metab 2020;40(9):1890–1901.
26. Eidelberg D, Moeller JR, Dhawan V, et al. The metabolic topography of parkinsonism. J Cereb Blood Flow Metab 1994;14(5): 783–801.
27. Ma Y, Tang C, Spetsieris PG, Dhawan V, Eidelberg D. Abnormal metabolic network activity in Parkinson's disease: test-retest reproducibility. J Cereb Blood Flow Metab 2007;27(3):597–605.
28. Teune LK, Renken RJ, de Jong BM, et al. Parkinson's disease-related perfusion and glucose metabolic brain patterns identified with PCASL-MRI and FDG-PET imaging. Neuroimage Clin 2014;5: 240–244.
29. Eidelberg D. Metabolic brain networks in neurodegenerative disorders: a functional imaging approach. Trends Neurosci 2009;32(10): 548–557.
30. Nicastro N, Holland N, Savulich G, et al. (11)C-UCB-J synaptic PET and multimodal imaging in dementia with Lewy bodies. Eur J Hybrid Imaging 2020;4(1):25.
31. Chen MK, Mecca AP, Naganawa M, et al. Comparison of [(11)C] UCB-J and [(18)F]FDG PET in Alzheimer's disease: a tracer kinetic modeling study. J Cereb Blood Flow Metab 2021;41(9):2395–2409.
32. Delva A, Michiels L, Koole M, Van Laere K, Vandenberghe W. Synaptic damage and its clinical correlates in people with early Huntington disease: a PET study. Neurology 2022;98(1):e83–e94.
33. Yousaf T, Dervenoulas G, Valkimadi PE, Politis M. Neuroimaging in Lewy body dementia. J Neurol 2019;266(1):1–26.
34. Saeed U, Compagnone J, Aviv RI, et al. Imaging biomarkers in Parkinson's disease and parkinsonian syndromes: current and emerging concepts. Transl Neurodegener 2017;6:8.
35. Poewe W, Seppi K, Tanner CM, et al. Parkinson disease. Nat Rev Dis Primers 2017;3:17013.
36. Gai WP, Halliday GM, Blumbergs PC, Geffen LB, Blessing WW. Substance P-containing neurons in the mesopontine tegmentum are severely affected in Parkinson's disease. Brain 1991;114(Pt 5):2253–2267.
37. German DC, Manaye KF, White CL 3rd, et al. Disease-specific patterns of locus coeruleus cell loss. Ann Neurol 1992;32(5):667–676.
38. Jellinger KA. Morphological substrates of mental dysfunction in Lewy body disease: an update. J Neural Transm Suppl 2000;59: 185–212.
39. Zarow C, Lyness SA, Mortimer JA, Chui HC. Neuronal loss is greater in the locus coeruleus than nucleus basalis and substantia nigra in Alzheimer and Parkinson diseases. Arch Neurol 2003;60(3): 337–341.
40. Agid Y, Graybiel AM, Ruberg M, et al. The efficacy of levodopa treatment declines in the course of Parkinson's disease: do non-dopaminergic lesions play a role? Adv Neurol 1990;53:83–100.
41. Frisina PG, Haroutunian V, Libow LS. The neuropathological basis for depression in Parkinson's disease. Parkinsonism Relat Disord 2009;15(2):144–148.
42. Jellinger KA. Pathology of Parkinson's disease. Changes other than the nigrostriatal pathway. Mol Chem Neuropathol 1991;14(3): 153–197.
43. Jellinger KA, Paulus W. Clinico-pathological correlations in Parkinson's disease. Clin Neurol Neurosurg 1992;94(Suppl): S86–S88.
44. Chan-Palay V. Galanin hyperinnervates surviving neurons of the human basal nucleus of Meynert in dementias of Alzheimer's and Parkinson's disease: a hypothesis for the role of galanin in accentuating cholinergic dysfunction in dementia. J Comp Neurol 1988; 273(4):543–557.
45. Kosaka K, Tsuchiya K, Yoshimura M. Lewy body disease with and without dementia: a clinicopathological study of 35 cases. Clin Neuropathol 1988;7(6):299–305.
46. Sudarsky L, Morris J, Romero J, Walshe TM. Dementia in Parkinson's disease: the problem of clinicopathological correlation. J Neuropsychiatry Clin Neurosci 1989;1(2):159–166.
47. Yoshimura M. Pathological basis for dementia in elderly patients with idiopathic Parkinson's disease. Eur Neurol 1988;28(Suppl 1): 29–35.
48. Uhl GR, Hedreen JC, Price DL. Parkinson's disease: loss of neurons from the ventral tegmental area contralateral to therapeutic surgical lesions. Neurology 1985;35(8):1215–1218.
49. Hirsch EC, Graybiel AM, Duyckaerts C, Javoy-Agid F. Neuronal loss in the pedunculopontine tegmental nucleus in Parkinson disease and in progressive supranuclear palsy. Proc Natl Acad Sci U S A 1987;84(16):5976–5980.
50. Jellinger K. The pedunculopontine nucleus in Parkinson's disease, progressive supranuclear palsy and Alzheimer's disease. J Neurol Neurosurg Psychiatry 1988;51(4):540–543.
51. Biesold D, Inanami O, Sato A, Sato Y. Stimulation of the nucleus basalis of Meynert increases cerebral cortical blood flow in rats. Neurosci Lett 1989;98(1):39–44.
52. Cudennec A, Bonvento G, Duverger D, Lacombe P, Seylaz J, MacKenzie ET. Effects of dorsal raphe nucleus stimulation on cerebral blood flow and flow-metabolism coupling in the conscious rat. Neuroscience 1993;55(2):395–401.
53. Leenders KL, Wolfson L, Gibbs JM, et al. The effects of L-DOPA on regional cerebral blood flow and oxygen metabolism in patients with Parkinson's disease. Brain 1985;108(1):171–191.
54. Underwood MD, Bakalian MJ, Arango V, Mann JJ. Effect of chemical stimulation of the dorsal raphe nucleus on cerebral blood flow in rat. Neurosci Lett 1995;199(3):228–230.
55. Borghammer P. Perfusion and metabolism imaging studies in Parkinson's disease. Dan Med J 2012;59(6):B4466.
56. Hilker R, Thomas AV, Klein JC, et al. Dementia in Parkinson disease: functional imaging of cholinergic and dopaminergic pathways. Neurology 2005;65(11):1716–1722.
57. Braak H, Rub U, Gai WP, Del Tredici K. Idiopathic Parkinson's disease: possible routes by which vulnerable neuronal types may be subject to neuroinvasion by an unknown pathogen. J Neural Transm 2003;110(5):517–536.
58. Braak H, Del Tredici K, Rub U, de Vos RA, Jansen Steur EN, Braak E. Staging of brain pathology related to sporadic Parkinson's disease. Neurobiol Aging 2003;24(2):197–211.
59. Aanerud J, Borghammer P, Chakravarty MM, et al. Brain energy metabolism and blood flow differences in healthy aging. J Cereb Blood Flow Metab 2012;32(7):1177–1187.
60. Borghammer P, Cumming P, Aanerud J, Gjedde A. Artefactual subcortical hyperperfusion in PET studies normalized to global mean: lessons from Parkinson's disease. Neuroimage 2009;45(2):249–257.
61. Asai M, Fujikawa A, Noda A, Miyoshi S, Matsuoka N, Nishimura S. Donepezil- and scopolamine-induced rCMRglu changes assessed by PET in conscious rhesus monkeys. Ann Nucl Med 2009;23(10):877–882.

Supporting Data

Additional Supporting Information may be found in the online version of this article at the publisher's web-site.

15318257, 2023, 5, Downloaded from https://movementdisorders.onlinelibrary.wiley.com/doi/10.1002/mds.29375 by Royal Danish Library, Wiley Online Library on [22/06/2023]. See the Terms and Conditions (https://onlinelibrary.wiley.com/terms-and-conditions) on Wiley Online Library for rules of use; OA articles are governed by the applicable Creative Commons License